efficiently when the C–Sn bond is orthogonal to the π-system.[15] Studies of medium ring systems incorporating metal substituents are currently being examined structurally and mechanistically, and these will be reported at a later date.

Acknowledgment. We are grateful to the Australian Research Grants Scheme, CNR (Roma), and the Ministero della Pubblica Istruzione (Roma) for financial support and to Professor David St. C. Black, University of New South Wales, for the acquisition of the 500-MHz NMR spectrum.

Registry No. 1, 14540-08-0; 2, 118893-17-7; $(C_6H_5)_3SnLi$, 4167-90-2; cyclohept-2-enyl chloride, 35021-99-9.

Supplementary Material Available: Tables of thermal parameters and hydrogen atom coordinates for 1 and 2 (4 pages); listings of structure factors for 1 and 2 (35 pages). Ordering information is given on any current masthead page.

Preparation, Characterization, and Structural Analyses of $[Rh(chp)(NBD)]_2$ and $[Rh(chp)(NBD)]_2(PF_6)$. Isolation of a Paramagnetic d^7–d^8 Binuclear Radical and Its d^8–d^8 Precursor

David C. Boyd, Robert Szalapski, and Kent R. Mann*

Department of Chemistry, University of Minnesota, Minneapolis, Minnesota 55455

Received August 4, 1988

Single-crystal X-ray studies of $[Rh(chp)(NBD)]_2$ and its one-electron oxidation product $[Rh(chp)(NBD)]_2PF_6{\cdot}CH_2Cl_2$ (chp = 6-chloro-2-hydroxypyridinate; NBD = norbornadiene) have been completed. Crystal data for $[Rh(chp)(NBD)]_2$ at 22 °C: space group $P2_1/c$; $Z = 4$; $a = 14.639$ (2) Å, $b = 10.483$ (3) Å, $c = 15.271$ (3) Å, $\beta = 103.04$ (2)°, $V = 2283$ (2) Å^3; $R = 0.024$, $R_w = 0.034$ for 3784 reflections with $F_o^2 > \sigma(F_o^2)$. Crystal data for $[Rh(chp)(NBD)]_2PF_6{\cdot}CH_2Cl_2$ at −72 °C: space group $P\bar{1}$; $Z = 2$; $a = 10.160$ (4) Å, $b = 12.770$ (5) Å, $c = 13.129$ (7) Å, $\alpha = 75.70$ (4)°, $\beta = 68.39$ (4)°, $\gamma = 67.94$ (3)°, $V = 1456.0$ (1.1) Å^3; $R = 0.061$, $R_w = 0.060$ for 3237 reflections with $F_o^2 > \sigma(F_o^2)$. $[Rh(chp)(NBD)]_2$ contains two square-planar Rh(I) units that intersect with a dihedral angle of 49° bridged by two hydroxypyridinate ligands. The molecule is structurally similar to the previously characterized $[Rh(mhp)(COD)]_2$ (mhp = 6-methyl-2-hydroxypyridinate; COD = 1,5-cyclooctadiene). The Rh–Rh distance is relatively short (3.040 (1) Å) for d^8d^8 complexes, which is consistent with our observations of a low-energy $d\sigma^* \rightarrow p\sigma$ electronic spectral band and its ease of oxidation. Addition of $AgPF_6$ to CH_2Cl_2 solutions produces the stable d^8d^7, mixed-valence complex $[Rh(chp)(NBD)]_2PF_6{\cdot}CH_2Cl_2$. This complex is paramagnetic ($\mu_{eff} = 1.76\ \mu_B$; EPR $g_1 = 2.08$, $g_2 = 2.21$, and $g_3 = 2.25$) and shows a broad signal for g_1 that is consistent with two equivalent $Rh(I^1/_2)$ atoms. The crystal structure of the d^8d^7 radical indicates that its geometry is similar to the d^8d^8 parent, but the Rh–Rh distance is considerably shorter (2.819 (1) Å). The shortening of the Rh–Rh distance is consistent with the $^1/_2$ bond order expected for a $(d\sigma_b)^2(d\sigma^*)^1$ electronic configuration in the radical.

Introduction

Binuclear complexes of rhodium and iridium undergo facile redox reactions that implicate them as catalytic electron-transfer agents.[1] Binuclear systems previously studied are capable of one- or two-electron oxidations that generate d^7–d^8 radical species,[2,3] or d^7–d^7 binuclear complexes.[4–6] Our previous studies have demonstrated that the thermodynamics of electron transfer are sensitive to factors such as structural changes and medium effects,[7] but the precise nature of these effects is largely unexplored.

Previous work[8–11] has centered on the properties of the d^8–d^8 complexes rather than the less stable, radical reaction intermediates. The combination of chp (chp = 6-chloro-2-hydroxypyridinate) as the bridging ligand and NBD (NBD = norbornadiene) has allowed the synthesis and structural examination of a reduced d^8–d^8 binuclear *and* the corresponding oxidized d^8–d^7 radical with identical ligation. This pair of complexes allows the influence of oxidation state on the metal–metal and metal–ligand interactions to be investigated.

Experimental Section

General Considerations. All synthetic procedures were carried out under an atmosphere of purified N_2 by using standard Schlenk techniques. Solvents used were of spectroscopic grade and used without further purification unless otherwise noted. Protonated hydroxypyridinates, cyclooctadiene, norbornadiene, $AgPF_6$, and $AgBF_4$ were purchased from Aldrich Chemical Co. The hydroxypyridines were converted to their corresponding sodium salts with sodium methoxide in methanol. $[Rh(NBD)Cl]_2$ was prepared by a published procedure.[12] NMR spectra were recorded on a Nicolet NT-300 WB instrument. Proton chemical shifts are reported relative to $Si(CH_3)_4$. Elemental analyses were performed by MHW Laboratories (Phoenix, AZ).

Synthesis. $[Rh(chp)(NBD)]_2$. A solution of 0.5454 g of $AgBF_4$ (2.80×10^{-3} mol) and 0.6460 g (1.40×10^{-3} mol) of [Rh-

* To whom correspondence should be addressed.

(1) Gray, H. B.; Miskowski, V. M.; Milder, S. J.; Smith, T. P.; Maverick, A. W.; Buhr, J. D.; Gladfelter, W. L.; Segal, I. S.; Mann, K. R. *Fundam. Res. Homogeneous Catal.* **1979**, *3*, 819.
(2) Boyd, D. C.; Matsch, P. A.; Mixa, M. M.; Mann, K. R. *Inorg. Chem.* **1986**, *25*, 3331.
(3) Miskowski, V. M.; Mann, K. R.; Gray, H. B.; Milder, S. J.; Hammond, G. S.; Ryason, P. R. *J. Am. Chem. Soc.* **1979**, *101*, 4383.
(4) Matsch, P. A. M. S. Thesis, University of Minnesota, 1985.
(5) Caspar, J. V.; Gray, H. B. *J. Am. Chem. Soc.* **1984**, *106*, 3029.
(6) Smith, T. P. Ph.D. Thesis, California Institute of Technology, 1982.
(7) Boyd, D. C.; Rodman, G. S.; Mann, K. R. *J. Am. Chem. Soc.* **1986**, *108*, 1779.
(8) Mixa, M. M. Ph.D. Thesis, University of Minnesota, 1985.
(9) Coleman, A. W.; Eadie, D. T.; Stobart, S. R.; Zaworotko, M. J.; Atwood, J. L. *J. Am. Chem. Soc.* **1982**, *104*, 922.
(10) Rodman, G. S.; Mann, K. R. *Inorg. Chem.*, in press.
(11) Rodman, G. S.; Mann, K. R. *Inorg. Chem.* **1985**, *24*, 3507.
(12) Abel, B. E.; Bennett, M. A.; Wilkinson, G. *J. Chem. Soc.* **1959**, 3178.

0276-7333/89/2308-0790$01.50/0

$(NBD)Cl]_2$ in 150 mL of acetonitrile was prepared. The yellow solution was stirred for 15 min to give $[Rh(NBD)(CH_3CN)_2]^+$ and AgCl. After filtration of the solid AgCl, Na(chp) (0.4265 g (2.81 $\times 10^{-3}$ mol)) dissolved in 100 mL of CH_3CN was added. The mixture was stirred 15 min to yield an orange solution with suspended orange solid. The solid was filtered and the mother liquor evaporated to dryness. The solids were combined, redissolved in a 9:1 CH_2Cl_2–acetone mixture, and eluted through a silica gel column. The elutant volume was reduced and the solution layered with CH_3CN to form 0.6250 g (9.66×10^{-4} mol) of microcrystalline $[Rh(chp)(NBD)]_2$ (69% yield). ^1H NMR (acetone-d_6, –91 °C): δ 7.052 (t, 1 H, chp); 6.305 (d, 1 H, chp); 6.013 (d, 1 H, chp); 4.771 (s, 1 H, NBD); 4.532 (s, 1 H, NBD); 4.332 (s, 1 H, NBD); 4.001 (s, 1 H, NBD); 3.528 (s, 1 H, NBD); 3.256 (s, 1 H, NBD); 1.277 (d, 1 H, NBD); 1.206 (d, 1 H, NBD). UV–vis (CH_2Cl_2 solution): λ_{max} 305 nm (ϵ_{max} 1.25×10^4 M^{-1} cm^{-1}), 476 (4.94×10^3 M^{-1} cm^{-1}). Anal. Calcd for $C_{24}H_{22}N_2O_2Cl_2Rh_2$: C, 44.54; H, 3.43; N, 4.33. Found: C, 44.33; H, 3.64; N, 4.32.

$[Rh(chp)(NBD)]_2(PF_6)$. A concentrated solution of 0.065 g of $[Rh(chp)(NBD)]_2$ (1.00×10^{-4} mol) dissolved in 4 mL of CH_2Cl_2 was prepared. To this solution was added 0.025 g (9.9×10^{-5} mol) of $AgPF_6$. As the oxidation proceeded, a dark green-brown solution was produced and metallic silver precipitated from the solution. The silver metal was filtered away and the solvent removed to yield a dark green-brown powder. The solid material was washed with hexane and recrystallized from CH_2Cl_2 and hexane producing 0.069 g (8.7×10^{-5} mol) of $[Rh(chp)(NBD)]_2(PF_6)$ (87.4%). UV–vis (CH_2Cl_2 solution): λ_{max} 392 nm (ϵ_{max} 4.43 $\times 10^3$ M^{-1} cm^{-1}), 440 (6.34×10^3), 529 (1.36×10^3), 720 (2.80×10^3). Magnetic moment: $\mu_{eff} = 1.76$ μ_B. Anal. Calcd for $[Rh(chp)(NBD)]_2(PF_6)\cdot CH_2Cl_2$ ($C_{25}H_{24}N_2O_2Cl_4PF_6Rh_2$): C, 34.23; H, 2.76; N, 3.19. Found: C, 34.55; H, 3.45; N, 3.31. EPR (frozen CH_2Cl_2/TBAP solution): $g_1 = 2.08$; $g_2 = 2.21$, $g_3 = 2.25$.

Instrumental Techniques. Electronic absorption spectra were recorded on either a Cary Model 17D spectrophotometer interfaced to a Zenith-150 microcomputer or a Tracor Northern TN-6500 rapid-scan diode-array spectrometer. Solvent background subtraction and plotting of the Cary data were performed with Lotus-123 software.

X-Band EPR spectra were recorded on a Varian Model E-3 spectrometer equipped with a nitrogen-flow temperature controller. The magnetic field in all EPR experiments was calibrated with the 2,2-diphenyl-1-picrylhydrazyl hydrate free radical (DPPH) as an internal standard ($g = 2.0037$).[13]

Magnetic moment data were collected with a Faraday system with $HgCo(SCN)_4$ as a calibrant.[14] Weight changes were measured at two field strengths and the results averaged. Diamagnetic corrections were estimated from Pascal's constants.[15]

Collection and Reduction of Crystallographic Data. General Considerations. Suitable crystals of $[Rh(chp)(NBD)]_2$ were obtained by layering a $CHCl_3$ solution of the complex with CH_3CN at room temperature. Crystals of $[Rh(chp)(NBD)]_2PF_6\cdot CH_2Cl_2$ were prepared similarly at 0 °C with a CH_2Cl_2/hexane solvent combination.

The automatic peak searching, centering, and indexing routines available on the Enraf-Nonius SDP-CAD4 automatic diffractometer[16] were used to find and center the reflections which were used to define the unit cell parameters. Space group assignments were made by examining the data collected for systematic absences and confirmed by the successful solution and refinement of the structures. Data processing and reduction,[17] Patterson function, Fourier and difference Fourier syntheses, and least-squares refinement[18] were carried out with the computer programs available in the Enraf-Nonius structure-solving package. Scattering factors were from Cromer and Waber[19] and included the effects of anomalous dispersion.[20] Summaries of the crystal data and

Table I. Crystal Data and Collection Parameters for $[Rh(chp)(NBD)]_2$ and $[Rh(chp)(NBD)]_2(PF_6)\cdot CH_2Cl_2$

	$C_{24}H_{22}Cl_2N_2O_2Rh_2$	$C_{25}H_{24}Cl_4F_6N_2O_2PRh_2$
fw	647.17	877.07
space group	$P2_1/c$	$P\bar{1}$
a, Å	14.639 (2)	10.160 (4)
b, Å	10.483 (3)	12.770 (5)
c, Å	15.271 (3)	13.129 (7)
α, deg	90.00	75.70 (4)
β, deg	103.04 (2)	68.39 (4)
γ, deg	90.00	67.94 (3)
V, Å^3	2282.9 (1.6)	1456.0 (1.1)
Z	4	2
d(calcd), g/cm^3	1.883	2.000
cryst size, mm	0.18 × 0.25 × 0.40	0.05 × 0.15 × 0.18
μ, cm^{-1}	16.8	16.1
radiatn (graphite monochromated)	Mo Kα (λ = 0.71073 Å)	
temp, °C	22	–72
scan type	ω–2θ	ω–2θ
collectn range, deg	2θ = 0–52	2θ = 0–48
no. of unique data	4721	4561
no. of data for $F^2 > \sigma(F^2)$	3784	3237
P	0.05	0.05
no. of variables	312	343
R	0.024	0.061
R_w	0.034	0.060
goodness of fit	1.037	1.298

Table II. Positional Parameters and Their Estimated Standard Deviations for $[Rh(chp)(NBD)]_2$

atom	x	y	z	B, Å^2
Rh1	0.15459 (1)	0.19146 (2)	0.10540 (1)	2.690 (4)
Rh2	0.30380 (2)	0.33964 (2)	0.03837 (1)	2.675 (4)
N1A	0.2784 (2)	0.0781 (2)	0.1531 (2)	2.68 (4)
C1A	0.3629 (2)	0.1359 (3)	0.1782 (2)	2.64 (5)
C2A	0.4406 (2)	0.0659 (3)	0.2255 (2)	3.43 (6)
C3A	0.4328 (2)	–0.0622 (3)	0.2397 (2)	3.95 (7)
C4A	0.3468 (3)	–0.1213 (3)	0.2099 (2)	4.14 (7)
C5A	0.2733 (2)	–0.0473 (3)	0.1686 (2)	3.33 (6)
O1A	0.3713 (1)	0.2543 (2)	0.1597 (1)	3.30 (4)
Cl5A	0.16270 (6)	–0.11564 (9)	0.13334 (7)	5.06 (2)
N1B	0.2969 (2)	0.1643 (2)	–0.0338 (2)	2.82 (5)
C1B	0.2157 (2)	0.0961 (3)	–0.0546 (2)	2.96 (6)
C2B	0.2119 (3)	–0.0162 (3)	–0.1066 (2)	4.12 (7)
C3B	0.2881 (3)	–0.0545 (3)	–0.1355 (2)	5.18 (8)
C4B	0.3699 (3)	0.0138 (4)	–0.1149 (3)	5.25 (8)
C5B	0.3695 (2)	0.1219 (3)	–0.0649 (2)	3.91 (7)
O1B	0.1143 (1)	0.1361 (2)	–0.0272 (1)	3.54 (4)
Cl5B	0.47142 (6)	0.2124 (1)	–0.03655 (9)	6.74 (3)
C1C	0.2076 (3)	0.5653 (3)	0.0114 (2)	4.05 (7)
C2C	0.2832 (2)	0.5198 (3)	0.0927 (2)	3.68 (7)
C3C	0.3664 (3)	0.5208 (3)	0.0643 (2)	3.86 (7)
C4C	0.3435 (2)	0.5673 (3)	–0.0335 (2)	4.10 (7)
C5C	0.2892 (2)	0.4494 (3)	–0.0784 (2)	3.41 (6)
C6C	0.2047 (2)	0.4483 (3)	–0.0505 (2)	3.29 (6)
C7C	0.2632 (3)	0.6600 (3)	–0.0323 (3)	5.01 (9)
C1D	0.0853 (2)	0.4016 (4)	0.1744 (2)	4.42 (7)
C2D	0.1637 (2)	0.3088 (3)	0.2175 (2)	3.64 (6)
C3D	0.1193 (2)	0.1953 (3)	0.2307 (2)	3.56 (6)
C4D	0.0150 (2)	0.2188 (4)	0.1970 (2)	4.36 (8)
C5D	0.0106 (2)	0.2264 (4)	0.0948 (2)	4.31 (8)
C6D	0.0548 (2)	0.3397 (4)	0.0826 (2)	4.15 (7)
C7D	0.0064 (2)	0.3595 (4)	0.2200 (3)	5.19 (9)

(13) Drago, R. S. *Physical Methods in Chemistry*; W. B. Saunders Co.: Philadelphia, 1977; p 324.

(14) Figgis, B. N.; Nyholm, R. S. *J. Chem. Soc.* **1958**, 4190.

(15) Lewis, J.; Wilkins, R. G. *Modern Coordination Chemistry*; Interscience Publishers: New York, 1960; p 403.

(16) All calculations were carried out on PDP 8A and 11/34 computers using the Enraf-Nonius CAD 4-SDP programs. This crystallographic computing package is described in the following references. Frenz, B. A. The Enraf-Nonius CAD 4 SDP-A Real Time System for Concurrent X-ray Data Collection and Crystal Structure Determination. In *Computing in Crystallography*, Schenk, H., Olthof-Hazekemp, R., van Koningsveld, H., Bassi, G. C., Eds.; Delft University Press: Delft, Holland, 1978; pp 64–71. In the CAD 4 SDP Users; Enraf–Nonius; Delft, Holland, 1978.

(17) The intensity data were processed as described previously. See: Bohling, D. A.; Mann, K. R. *Inorg. Chem.* **1984**, *23*, 1426.

(18) The function minimized was $w(F_o - F_c)^2$ where $w = 1/\sigma^2(F_o)$. The unweighted and weighted residuals are defined in the usual way: see ref 17.

(19) Cromer, D. T.; Waber, J. T. *International Tables for X-Ray Crystallography*; Kynoch Press: Birmingham, England, 1974; Vol. IV, Table 2.2.4 Cromer, D. t. *Ibid.* Table 2.3.1.

Table III. Positional Parameters and Their Estimated Standard Deviations for $[Rh(chp)(NBD)]_2(PF_6)\cdot CH_2Cl_2$

atom	x	y	z	B, Å²
Rh1	0.38952 (8)	0.24355 (6)	0.08650 (6)	1.48 (2)
Rh2	0.18423 (8)	0.13322 (6)	0.23298 (6)	1.53 (2)
O1A	0.1327 (7)	0.2658 (6)	0.3164 (6)	3.2 (2)
C1A	0.237 (1)	0.2925 (7)	0.3255 (8)	1.8 (2)
N1A	0.3629 (8)	0.2869 (6)	0.2378 (6)	1.8 (2)
C2A	0.225 (1)	0.3286 (9)	0.4235 (9)	2.9 (3)
C3A	0.341 (1)	0.3538 (8)	0.4274 (9)	3.0 (3)
C4A	0.470 (1)	0.3459 (9)	0.3392 (9)	3.0 (3)
C5A	0.474 (1)	0.3153 (8)	0.2473 (8)	2.1 (2)
Cl5A	0.6270 (3)	0.3043 (2)	0.1293 (2)	2.89 (7)
O1B	0.5281 (6)	0.0825 (5)	0.1133 (5)	2.2 (2)
C1B	0.5120 (9)	0.0293 (7)	0.2128 (8)	1.6 (2)
N1B	0.3729 (8)	0.0442 (6)	0.2846 (6)	1.6 (2)
C2B	0.637 (1)	−0.0424 (8)	0.2475 (8)	2.1 (2)
C3B	0.616 (1)	−0.0977 (9)	0.3527 (9)	2.8 (3)
C4B	0.472 (1)	−0.081 (1)	0.4264 (9)	3.0 (3)
C5B	0.358 (1)	−0.0116 (9)	0.3878 (8)	2.4 (3)
C65B	0.1742 (3)	0.0126 (3)	0.4711 (2)	3.51 (8)
C1C	0.090 (1)	0.1095 (8)	0.0685 (7)	1.7 (2)
C2C	0.0200 (9)	0.2033 (8)	0.1438 (8)	1.9 (2)
C3C	−0.043 (1)	0.1540 (9)	0.2459 (8)	2.3 (2)
C4C	−0.014 (1)	0.0302 (8)	0.2389 (8)	2.0 (2)
C5C	0.156 (1)	−0.0184 (8)	0.2169 (8)	2.3 (2)
C6C	0.220 (1)	0.0311 (8)	0.1135 (8)	1.9 (2)
C7C	−0.021 (1)	0.0414 (8)	0.1222 (8)	2.2 (2)
C1D	0.229 (1)	0.3406 (9)	−0.0652 (9)	2.6 (3)
C2D	0.216 (1)	0.3843 (8)	0.0386 (8)	2.0 (2)
C3D	0.343 (1)	0.4160 (8)	0.0136 (8)	2.5 (3)
C4D	0.435 (1)	0.3902 (8)	−0.1072 (9)	2.4 (3)
C5D	0.485 (1)	0.2585 (8)	−0.0911 (8)	2.1 (3)
C6D	0.360 (1)	0.2299 (8)	−0.0658 (8)	2.0 (2)
C7D	0.309 (1)	0.4172 (9)	−0.1568 (9)	2.9 (3)
P	0.0744 (3)	−0.3273 (2)	0.2138 (2)	2.58 (7)
F1	−0.0661 (8)	−0.228 (7)	0.1928 (6)	5.3 (2)
F6	0.2200 (8)	−0.4268 (7)	0.2305 (7)	5.9 (2)
Cl1S	0.7681 (4)	0.4279 (3)	0.3924 (3)	4.23 (9)
Cl2S	0.6517 (4)	0.2920 (4)	0.5929 (4)	6.5 (1)
CS	0.801 (1)	0.346 (1)	0.5130 (9)	3.3 (3)
F1D	−0.014	−0.350	0.337	4.2 (5)*
F2D	0.023	−0.303	0.335	4*
F3D	0.074	−0.264	0.300	4*
F4D	0.125	−0.241	0.243	4*
F5D	0.162	−0.241	0.177	4*
F6D	0.176	−0.264	0.121	4*
F7D	0.162	−0.304	0.091	4*
F8D	0.125	−0.351	0.093	4*
F9D	0.074	−0.391	0.128	4*
F10D	0.024	−0.414	0.185	4*
F11D	−0.014	−0.413	0.251	4*
F12D	−0.027	−0.390	0.307	4*

collection parameters for the complexes are found in Table I.

Both structures were solved from the three-dimensional Patterson function which allowed placement of the rhodium atoms. Fourier and difference Fourier analyses in conjunction with cycles of least-squares refinement[19] allowed placement of the remaining atoms, excluding the hydrogen atoms. Full matrix least-squares refinment utilized anisotropic temperature factors for all non-hydrogen atoms. Hydrogen atoms were placed at idealized positions, and their isotropic temperature factors allowed to vary as a test of the model; they refined to reasonable values.

$[Rh(chp)(NBD)]_2$. No decrease or fluctuations were observed in check reflections taken during data collection. The space group $P2_1/c$ (No. 14) was indicated by the systematic absences in the data. An empirical correction was made for absorption (μ = 16.8 cm^{-1}). Convergence occurred at R = 0.024 and R_W = 0.034. The error in an observation of unit weight was 1.037 with the use of a value of 0.05 for p in the $\sigma(I)$ equation.[17] Tables II and IV contain the final positional parameters and selected bond lengths. The final thermal parameters, hydrogen positions, other bond lengths and bond angles, a summary of the least-squares planes, and the calculated and observed structure factors are included as supplementary material.

Table IV. Selected Bond Distances[a] for $[Rh(chp)(NBD)]_2$ and $[Rh(chp)(NBD)]_2PF_6\cdot CH_2Cl_2$

bond	$[Rh(chp)(NBD)]_2$	$[Rh(chp)(NBD)]_2PF_6\cdot CH_2Cl_2$	Δd[b,c]
Rh1–Rh2	3.040 (1)	2.819 (1)	−0.221 (1)
Rh1–N1A	2.152 (2)	2.088 (7)	−0.064 (7)
Rh1–O1B	2.079 (2)	2.042 (6)	−0.037 (6)
Rh1–C2D	2.088 (3)	2.145 (9)	+0.057 (9)
Rh1–C3D	2.093 (3)	2.121 (9)	+0.028 (9)[d]
Rh1–C5D	2.110 (3)	2.161 (9)	+0.051 (9)
Rh1–C6D	2.107 (3)	2.041 (6)	+0.079 (7)
Rh2–O1A	2.093 (2)	2.041 (6)	−0.052 (6)
Rh2–N1B	2.134 (2)	2.089 (7)	−0.045 (7)
Rh2–C2C	2.111 (3)	2.180 (9)	+0.069 (9)
Rh2–C3C	2.107 (3)	2.170 (9)	+0.063 (9)
Rh2–C5C	2.092 (3)	2.130 (9)	+0.038 (9)[e]
Rh2–C6C	2.087 (3)	2.129 (9)	+0.042 (9)[e]

[a] Bond distances in angstroms. Estimated standard deviations in the last significant digit are in parentheses. [b] Δd = d([Rh(chp)(NBD)]$_2$PF$_6$·CH$_2$Cl$_2$) − d([Rh(chp)(NBD)]$_2$). [c] All bond length changes exceed 5 esd except as noted. [d] Exceeds 3 esd. [e] Exceeds 4 esd.

$[Rh(chp)(NBD)]_2(PF_6)\cdot CH_2Cl_2$. During data collection, the check reflections showed a minimal decrease (0.2%) which did not require correction. The space groups $P1$ or $P\bar{1}$ (No. 2) were indicated by the data, with successful refinement in $P\bar{1}$. An empirical correction was made for absorption (μ = 16.1 cm^{-1}).

The structure was solved from the three-dimensional Patterson function which allowed placement of the rhodium atoms. Fourier and difference Fourier analyses in conjunction with cycles of least-squares refinement[18] allowed placement of the remaining atoms, excluding the hydrogen atoms and equatorial fluorine atoms of the disordered PF_6^- anion. Full-matrix least-squares refinement (343 variables) utilized anisotropic temperature factors for all non-hydrogen atoms and idealized placement of the hydrogen atoms with temperature factors (B) fixed at 3.0 Å² (B = 6.0 Å² for CH_2Cl_2).

Well-resolved peaks were observed for the phosphorus and axial fluorine atoms of the PF_6^- anion while the four equatorial fluorine atoms were disordered. The well-resolved atoms were refined anisotropically. The equatorial fluorine atoms were modeled with twelve $^1/_3$ occupancy atoms at fixed positions 1.55 Å from the phosphorus atom. Fixed temperature factors (B) of 4.0 Å² were used for these atoms.

Tables III contain the final positional parameters and selected bond lengths. The final thermal parameters, hydrogen positions, other bond lengths and bond angles, a summary of the least-squares planes, and the calculated and observed structure factors are included as supplementary material.

Results and Discussion

Characterization and Structural Analysis of $[Rh(chp)(NBD)]_2$. The room-temperature reaction of $[Rh(NBD)Cl]_2$ with the anion of 6-chloro-2-hydroxypyridinate (chp) results in the rapid formation of the orange product $[Rh(chp)(NBD)]_2$. The binuclear nature of the orange complex in the solid state was verified by standard characterization techniques including X-ray crystallography. This structure persists in solution as confirmed by ^1H NMR data and parallels the behavior of $[Rh(mhp)(COD)]_2$ (mhp = 6-methyl-2-hydroxypyridinate; COD = 1,5-cyclooctadiene).[10]

The structure of $[Rh(chp)(NBD)]_2$ (Figure 1) is composed of bridged, binuclear molecules with distorted square-planar arrangements of ligands around each of the Rh(I) metal centers. Each of the rhodium centers is bound to the nitrogen atom of a bridging chp, the oxygen atom of the other chp ligand, and a chelating norbornadiene group. The L–M–L bond angles in the coordination sphere of the molecule deviate from the idealized value of 90° due

(20) Cromer, D. T.; Ibers, J. A. *International Tables for X-Ray Crystallography*; Kynoch Press: Birmingham, England, 1974; Vol. IV.

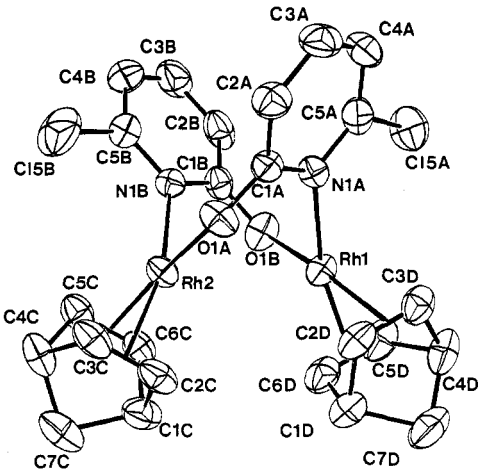

Figure 1. ORTEP drawing of [Rh(chp)(NBD)]$_2$ showing the atomic numbering scheme. Thermal ellipsoids are at 50% probability level.

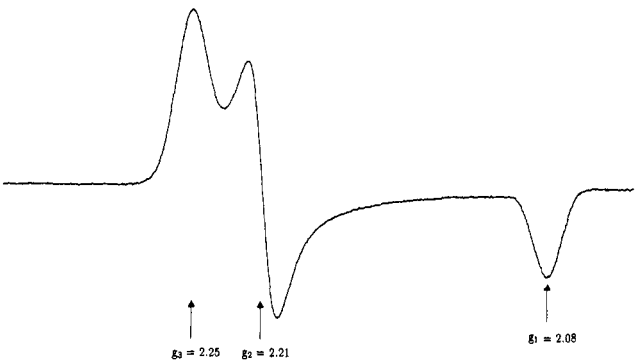

Figure 2. X-Band EPR spectrum of [Rh(chp)(NBD)]$_2^+$ at −160 °C in CH_2Cl_2/TBAP solution. Scan is from 2850 to 3350 G, and the frequency is 9.42 GHz.

to the small bite angle of the norbornadiene ligands (vide infra). The molecule has approximate C_2 symmetry with the pseudo C_2 axis lying between the two bridging chp ligands and bisecting the metal–metal axis.

The metal–ligand bond lengths for [Rh(chp)(NBD)]$_2$ are quite similar to those observed for [Rh(mhp)(COD)]$_2$,[10] with average Rh–O and Rh–N distances of 2.086 (3) and 2.143 (3) Å, respectively, in the NBD complex and 2.079 (3) and 2.132 (3) Å, respectively, in the COD complex. In each case, the slightly shorter Rh–O bond lengths may reflect the greater π-donating ability of the oxygen centers of the hydroxypyridinate ligands compared to the nitrogen centers. The Rh–NBD bond lengths are similar to the Rh–COD bond lengths of [Rh(mhp)(COD)]$_2$ but exhibit a slight trans influence. The Rh–C bonds trans to oxygen average 2.090 (4) Å, while the Rh–C bonds trans to a nitrogen atom of chp average 2.109 (4) Å.

The internal bonding of the NBD and chp ligands is not unusual in any discernible way. Comparisons of [Rh(chp)(NBD)]$_2$, [Rh(mhp)(COD)]$_2$, and [Rh(μ-OAC)(NBD)]$_2$ (μ-OAC = bridging acetate)[21] reveal comparable bond lengths and angles in all cases. The bite distance between the double bonds (center-to-center double-bond distance) is significantly different for the two dienes (2.340 (7) Å for NBD versus 2.770 (7) Å for COD), because NBD has a single bridgehead carbon atom separating the double bonds from one another, while COD has two atoms between the double bonds.

Table V. Metal–Centroid Data for Selected Complexes[a]

complex	M1–cent.1, Å	M2–cent.2, Å	M1–M2–cent.2,[b] deg	M2–M1–cent.1,[b] deg
[Ir(mhp)(COD)]$_2$[c]	1.42 (3)	1.43 (3)	126 (1)	125 (1)
[Rh(mhp)(COD)]$_2$[c]	1.43 (3)	1.43 (3)	126 (1)	126 (1)
[Rh(chp)(NBD)]$_2$	1.60 (3)	1.60 (3)	120 (1)	118 (1)
[Rh(chp)(NBD)]$_2^+$	1.66 (3)	1.66 (3)	117 (1)	117 (1)
[Rh(OAc)(NBD)]$_2$[d]	1.60 (3)	1.59 (3)	123 (1)	116 (1)

[a] Centroid (cent.) is the center of the plane defined by the four diene carbon atoms. M–centroid distances in angstroms and angles in degrees. [b] M–M–cent. is the angle formed by the metal–metal axis and the metal-centroid vector. [c] Reference 10. [d] Reference 23.

The bite angle of the NBD group is smaller relative to COD (72.4 (2)° in [Rh(chp)(NBD)]$_2$ versus 88.0 (2)° for [Rh(mhp)(COD)]$_2$) as defined by the L–M–L angle (the position of L is the center of the C=C double bonds). As a result of the relatively small L–M–L angle imposed by the NBD ligands, the O–Rh–L and N–Rh–L angles of the coordination core open (97.4 (1)°) beyond the idealized 90°, but the O–Rh–N angles of the chp ligands are relatively unaffected (92.7 (1)°). The comparable O–Rh–N and O–Rh–L angles for [Rh(mhp)(COD)]$_2$ are 90.4 (1)° and 90.6 (1)°, respectively.

The Rh–C distances in [Rh(chp)(NBD)]$_2$ and [Rh(mhp)(COD)]$_2$ are identical (2.100 (6) Å versus 2.103 (6) Å for the COD complex). In order to accommodate the ~2.1-Å Rh–C distance and the smaller bite distance of NBD, the metal–centroid distance (the centroid of the NBD is the center of the plane containing the alkene carbon atoms C2D, C3D, C5D, and C6D of [Rh(chp)(NBD)]$_2$) is approximately 0.2 Å longer in [Rh(chp)(NBD)]$_2$ than [Rh(mhp)(COD)]$_2$. A summary of the metal–centroid distances for several pertinent complexes are summarized in Table V.

The square planes established at each metal center intersect one another in a manner similar to the "open book" binuclear complexes [M(μ-pz)(COD)]$_2$ (M = Rh, Ir)[8,22] but are slightly skewed relative to one another. To describe this distortion, a "twist angle" that is similar to the torsional angle about the M–M bond in "face to face" complexes has been defined as the angle formed by the two intersecting planes (CT1–Rh1–Rh2 and Rh1–Rh2–CT2 where CT1 and CT2 are the centroids of the corresponding four alkene carbon atoms. The "twist angles" of [Rh(chp)(NBD)]$_2$, [Rh(mhp)(COD)]$_2$, and [Rh(OAc)(NBD)]$_2$ are of similar magnitude, (31(1)°, 25(1)°, and 25(1)° respectively).

The dihedral angle between the square planes of [Rh(chp)(NBD)]$_2$ is 49.0°, significantly smaller than analogous COD complex ([Rh(mhp)(COD)]$_2$ = 57.2°[10] and [Rh(pz)(COD)]$_2$ = 80.7°)[22] but similar to another NBD complex with acetate bridges, [Rh(OAc)(NBD)]$_2$ (50.1°).[21] The large dihedral angle of the pyrazolyl-bridged species is a result of the six-membered ring in the μ-pz system and the larger steric requirements of COD relative to NBD.

Electronic differences between the individual C=C bonds in NBD and COD are negligible, so that the observed differences in dihedral angle observed for [Rh(mhp)(COD)]$_2$ and [Rh(chp)(NBD)]$_2$ are ascribed to the relative steric requirements of the two diene ligands. The smaller NBD ligand with longer M–C distances allows a smaller dihedral angle between the square planes which decreases in the NBD complex and allows a substantial

(21) Reis, A. H.; Willi, C.; Siegel, S.; Tani, B. *Inorg. Chem.* **1979**, *18*, 1859.

(22) Beveridge, K. A.; Bushnell, G. W.; Stobart, S. R.; Atwood, J. L.; Zaworotko, M. J. *Organometallics* **1983**, *2*, 1447.

(0.327 Å) decrease in the metal–metal distance as well. The metal–metal distance of $[Rh(chp)(NBD)]_2$ is 3.040 (1) Å compared to 3.367 (1) Å for $[Rh(mhp)(COD)]_2$[10] and 3.267 (1) Å for $[Rh(pz)(COD)]_2$.[22] The acetate-bridged, NBD species $[Rh(OAc)(NBD)]_2$ displays a Rh–Rh distance of 3.105 (1) Å,[21] more comparable to $[Rh(chp)(NBD)]_2$ than $[Rh(mhp)(COD)]_2$. The data show a significant shortening of the metal–metal distance in the NBD complexes over the COD complexes. The shortening of the metal–metal distance enhances the metal–metal interaction and results in an unusually low-energy $d\sigma^* \rightarrow p\sigma$ transition in comparison to the COD complex. The NBD complex exhibits the $d\sigma^* \rightarrow p\sigma$ transition at 476 nm, while an analogous band in the COD complex occurs at 420 nm. The increased energy of the HOMO in the NBD complex must in part be responsible for the successful oxidation of the compound to the d^8d^7 radical because the corresponding COD complex radical is discernibly less stable.[23]

Characterization and Structural Analysis of $[Rh(chp)(NBD)]_2(PF_6)\cdot CH_2Cl_2$. Oxidation of $[Rh(chp)(NBD)]_2$ with $AgPF_6$ produces a green-brown paramagnetic complex, isolated as the PF_6^- salt. The elemental analysis of the green-brown solid is consistent with its formulation as a CH_2Cl_2 solvate, $[Rh(chp)(NBD)]_2(PF_6)\cdot CH_2Cl_2$. Electrochemical studies indicate the oxidation is a simple, one-electron process that generates the EPR-active cation radical $[Rh(chp)(NBD)]_2^+$. A magnetic moment determination of the green-brown material yielded $\mu_{eff} = 1.76$ μ_B, in accord with the presence of one unpaired electron per binuclear unit.

The frozen solution EPR spectrum of $[Rh(chp)(NBD)]_2^+$ generated in CH_2Cl_2/TBAP is composed of three relatively broad signals (g_1, g_2, g_3) consistent with a metal-centered, unpaired electron. The low symmetry of $[Rh(chp)(NBD)]_2^+$ ($\sim C_2$) produces one EPR signal for each of the three molecular axes. In previously assigned "face-to-face" compounds[2] the first signal appears as a triplet due to hyperfine coupling of the unpaired electron to two equivalent $I = {}^1/_2$ rhodium centers and corresponds to the metal–metal principal axis. The three line hyperfine pattern in these compounds indicates the unpaired electron is delocalized equally over both metal centers on the EPR time scale as has been previously observed for other dirhodium radical species. In the CHP complex, this triplet is not resolved ($g = 2.08$). However, in the closely related mhp complex (mhp = 6-methylhydroxypyridine) the three-line pattern is observed.[23] The other two signals at $g_2 = 2.21$ and $g_3 = 2.25$ are due to the two other components of the g tensor that lie in the plane perpendicular to the Rh–Rh vector.

To fully document the structural parameters of the d^8d^7 radical, a structural analysis of the paramagnetic complex was carried out at −72 °C. A summary of selected bond lengths are tabulated in Table IV. The main features of the $[Rh(chp)(NBD)]_2^+$ cation are similar to the reduced form. Both molecules have approximate C_2 symmetry, approximate square-planar geometry at the rhodium centers, and a coordination core of nitrogen, oxygen, and a diene group. Although several significant bond length changes accompany the one-electron oxidation, few significant bond angle changes result.

The one-electron oxidation of $[Rh(chp)(NBD)]_2$ removes one electron from the $d\sigma^*$ level and results in an increase in the formal bond order from 0 to ${}^1/_2$ between the rhodium centers.[24] This obnd order change is accompanied by a 0.221-Å decrease in metal–metal distance to 2.819 (1) Å but only a slight decrease in the dihedral angle between the square planes from 49.0° to 44.3°. The twist angle does not change upon oxidation (31°). The closer approach of the two metal centers on oxidation indicates that the Rh–Rh ${}^1/_2$ order metal–metal bond is substantial in the complex.

The structural changes observed upon oxidation of $[Rh(chp)(NBD)]_2$ are similar to those reported for a related dirhodium complex, $[Rh(CO)(PPh_3)(\mu\text{-RNNNR})]_2$ (PPh_3 = triphenylphosphine; μ-RNNNR = bridging triazenido with R = *p*-tolyl).[25] The chp ligand is similar to the triazenido ligand which also has a three-atom bridging group that coordinates to rhodium through the two nitrogen atoms. The Rh–Rh distance and dihedral angle in the neutral triazenido complex (2.960 (4) Å and 40.8°) are slightly smaller than those in $[Rh(chp)(NBD)]_2$ and change similarly on oxidation. The removal of one electron in this case also results in a paramagnetic complex with a metal–metal distance and dihedral angle of 2.698 (1) Å and 31.3°. The change in metal–metal distance (0.262 Å) in this case is similar to that observed upon oxidation of $[Rh(chp)(NBD)]_2$ (0.221 Å), but the dihedral angle of the triazenido-bridged complex decreases substantially (9.5° versus 4.7°). The smaller dihedral angle and shorter metal–metal distance in the triazenido complex result from more efficient staggering of the transoid PPh_3 groups. Staggering the bidentate NBD groups is not an effective method of relieving the similar steric interactions in $[Rh(chp)(NBD)]_2$ because of the larger steric bulk near the metal for NBD.

Several rhodium–ligand bond length changes are observed when $[Rh(chp)(NBD)]_2$ is oxidized to $[Rh(chp)(NBD)]_2^+$. The rhodium–chp bond lengths shorten (Rh–O and Rh–N bond lengths decrease by ~0.045 and 0.055 Å, respectively), but the rhodium–NBD bond lengthen (Rh–C_{diene} distances increase an average of 0.053 Å) when the neutral is oxidized. These bond length changes are consistent with the donor–acceptor qualities of each ligand group. In the oxidized complex, the metal centers form stronger interactions with predominantly π-donor groups (chp), but weaker interactions with predominantly π-acceptor groups (NBD). An extensive list of these and other bond length changes that result upon oxidation of $[Rh(chp)(NBD)]_2$ are in Table IV.

An intriguing comparison of structural changes can also be made between the one electron oxidation observed for $[Rh(chp)(NBD)]_2$ and the more commonly observed two electron oxidation in the face-to-face d^8-d^8 binuclears. Two electron oxidation of binuclear face-to-face d^8-d^8 complexes is usually accompanied by coordination of ligand groups in the axial sites of the square planes.[4-6,26,27] In contrast, the crystal structure of $[Rh(chp)(NBD)]_2(PF_6)\cdot CH_2Cl_2$ reveals the axial sites are *not* occupied by ligands, although the PF_6^- anion and CH_2Cl_2 of crystallization are positioned along the axial sites of the cation. The closest Rh2–P distance is 6.46 Å, which gives the shortest possible Rh–F distance of 4.89 Å, while the nearest Rh1–Cl distance is 6.92 Å. Neither of these distances could be considered bonding and are consistent with room-temperature solution measurements that previously[2,7] suggested that the d^8–d^7 radicals do not appreciably bind axial ligands. Apparently the occupation of $d\sigma^*$ by a single electron localizes

(23) Boyd, D. C. Ph.D. Thesis, University of Minnesota, 1987.
(24) This discussion is based on a model previously developed: Mann, K. R.; Gordon, J. G. II; Gray, H. B. *J. Am. Chem. Soc.* **1975**, *97*, 3553.
(25) Connelly, N. G.; Finn, C. J.; Freeman, M. J.; Orpen, A. G.; Sterling, J. *J. Chem. Soc., Chem. Commun.* **1984**, 1025.
(26) Marshall, J. L.; Stiegman, A. E.; Gray, H. B. *ACS Symp. Ser.* **1986**, *No. 307*, 166.
(27) Mann, K. R.; Bell, R. A.; Gray, H. B. *Inorg. Chem.* **1979**, *18*, 2671.

enough electron density in the axial positions to preclude coordination of axial ligands. Another point of contrast in the d^8d^7 structure versus d^7d^7 structures is the short RhRh distance. The RhRh bond (bond order $^1/_2$) in $[Rh(chp)(NBD)]_2^+$ (2.819 Å) is shorter than the RhRh (bond order 1) distance in $Rh_2(bridge)_4Cl_2^{2+}$ (2.837 Å) bridge = 1,3-diisocyanopropane). We attribute this apparent anomaly to a lenghthened Rh(II)–Rh(II) bond in the d^7d^7 bridge complex due to destabilization of the metal–metal bond via Rh–Cl axial bond formation.

Conclusions

The complex $[Rh(chp)(NBD)]_2$ has been prepared via a procedure previously found convenient for the preparation of $[Rh(hp)(COD)]_2$ and $[Ir(hp)(COD)]_2$. The neutral d^8–d^8 complex was isolated, characterized, and subjected to crystallographic analysis. $[Rh(chp)(NBD)]_2$ is composed of two intersecting square-planar Rh(I) centers bridged by the two hydroxypyridinate ligands. The molecule is structurally similar to the previously characterized $[M(mhp)(COD)]_2$ (M = Rh, Ir) complexes with nearly C_2 symmetry at the metals. The complex contains a relatively flexible eight-membered metallocycle ring and a shorter and stronger Rh–Rh interaction than the mhp complex. The smaller bite distance and steric requirements of NBD allow the Rh atoms to interact more strongly and allow the square planes to attain a dihedral angle of 49°.

The one-electron oxidation of $[Rh(chp)(NBD)]_2$ results in the formation of a stable radical complex, $[Rh(chp)(NBD)]_2^+$, that has been thoroughly characterized as a mixed-valence, paramagnetic complex. Crystallographic analysis indicates the removal of an electron from the metal–metal σ^* antibonding molecular orbital decreases the metal–metal distance to 2.819 Å, consistent with a bond order of one-half. The EPR spectrum of frozen CH_2Cl_2/TBAP solutions of $[Rh(chp)(NBD)]_2(PF_6)$ displays three signals at g = 2.08, 2.21, and 2.25 which correspond to random alignment of each molecular axis with the applied magnetic field.

Acknowledgment. We wish to thank Professor J. D. Britton for his expert assistance in the X-ray structure determinations and Johnson-Matthey for loans of rhodium and iridium trichlorides. The X-ray diffractometer was purchased in part through funds provided by National Science Foundation Grant CHE77-28505.

Registry No. $[Rh(chp)(NBD)]_2$, 118317-86-5; $[Rh(chp)(NBD)]_2(PF_6)$, 118299-44-8; $[Rh(NBD)Cl]_2$, 12257-42-0; Na(chp), 59432-71-2.

Supplementary Material Available: Tables of thermal parameters, hydrogen positions, bond lengths, bond angles, and least-squares planes (14 pages); listings of structure factors for $[Rh(chp)(NBD)]_2$ and $[Rh(chp)(NBD)](PF_6)\cdot CH_2Cl_2$ (29 pages). Ordering information is given on any current masthead page.

Reactions of Iridium(I) Alkoxide Complexes with Acyl and Alkyl Sources: Carbon–Oxygen Bond-Forming Reactions

Karen A. Bernard and Jim D. Atwood*

Department of Chemistry, University at Buffalo, State University of New York, Buffalo, New York 14214

Received August 5, 1988

The reactions of alkoxyiridium complexes *trans*-$ROIr(CO)(PPh_3)_2$ (R = Me, Ph, *t*-Bu, *i*-Pr) with organic substrates R′X (R′ = Me, $CH_3C(O)$, $C_6H_5C(O)$, $C_6H_5CH_2C(O)$, HC(O); X = Cl, I, H) lead to esters ROR′ but not to ethers. Reaction of acid chlorides leads to $R'Ir(CO)(PPh_3)_2Cl_2$ and the ester. Reaction of aldehydes gives $HIr(CO)_2(PPh_3)_2$ and the ester ROR′ in addition to Tischenko products $R'CH_2C(O)OR'$. Reaction of MeI gives the six-coordinate adduct $MeOIr(Me)(I)(CO)(PPh_3)_2$ that does not eliminate dimethyl ether. Carbonylation and decomposition of $MeOIr(Me)(I)(CO)(PPh_3)_2$ leading to $MeOC(O)Ir(Me)(I)(CO)(PPh_3)_2$ and *trans*-$Ir(CO)(PPh_3)_2I$, respectively, are also reported.

Bond formation through reductive elimination is an important reaction in organometallic chemistry and homogeneous catalysis. Carbon–hydrogen and, to a lesser extent, carbon-carbon bond formation have been examined.[1-11] Relatively few studies of oxygen–hydrogen and oxygen–carbon bond formation have appeared.[12-15] Oxidative additions to *trans*-$MeOIr(CO)(PPh_3)_2$ offer the potential to examine the systematics of carbon–oxygen and oxygen–hydrogen bond formation.

We have previously reported carbon–oxygen bond formation by addition of acid chlorides to *trans*-$ROIr(CO)(PPh_3)_2$

$$\textit{trans}\text{-}ROIr(CO)(PPh_3)_2 + 2R'C(O)Cl \rightarrow R'C(O)Ir(CO)(PPh_3)_2Cl_2 + R'C(O)OR \quad (1)$$

R = Me, Ph; R′ = Me, $CH_2C_6H_5$

which lead to ester formation.[14] Esters were also observed as products by addition of aldehydes to the iridium alkoxides[15]

(1) Halpern, J. *Acc. Chem. Res.* **1982**, *15*, 332.
(2) Norton, J. R. *Acc. Chem. Res.* **1979**, *12*, 139.
(3) Buchanan, J. M.; Stryker, J. M.; Bergman, R. G. *J. Am. Chem. Soc.* **1986**, *108*, 1537.
(4) Jones, W. D.; Bergman, R. G. *J. Am. Chem. Soc.* **1979**, *101*, 5447.
(5) Milstein, D. *J. Am. Chem. Soc.* **1982**, *104*, 5226.
(6) Ruszczyk, R. J.; Huang, B. L.; Atwood, J. D. *J. Organomet. Chem.* **1986**, *299*, 205.
(7) Gillie, A.; Stille, J. K. *J. Am. Chem. Soc.* **1980**, *102*, 4933.
(8) Komiya, S.; Shibae, A. *Organometallics* **1985**, *4*, 684.
(9) Smith, G.; Kochi, J. K. *J. Organomet. Chem.* **1980**, *198*, 199.
(10) Parshall, G. W. *J. Am. Chem. Soc.* **1974**, *96*, 2360.
(11) Ruddick, J. D.; Shaw, B. L. *J. Chem. Soc. A* **1969**, 2969.
(12) Goeden, G. V.; Caulton, K. G. *J. Am. Chem. Soc.* **1981**, *103*, 7354.
(13) Komiya, S.; Akai, Y.; Tanaka, K.; Yamamoto, T.; Yamamoto, A. *Organometallics* **1985**, *4*, 1130.
(14) Bernard, K. A.; Atwood, J. D. *Organometallics* **1987**, *6*, 1133.
(15) Bernard, K. A.; Atwood, J. D. *Organometallics* **1988**, *7*, 235.

0276-7333/89/2308-0795$01.50/0